PROCEEDINGS OF SPIE

SPIEDigitalLibrary.org/conference-proceedings-of-spie

Optoacoustic visualization of GCaMP6f labeled deep brain activity in a murine intracardiac perfusion model

Degtyaruk, Oleksiy, McLarney, Benedict, Deán-Ben, Xosé Luís, Shoham, Shy, Razansky, Daniel

Oleksiy Degtyaruk, Benedict McLarney, Xosé Luís Deán-Ben, Shy Shoham, Daniel Razansky, "Optoacoustic visualization of GCaMP6f labeled deep brain activity in a murine intracardiac perfusion model," Proc. SPIE 11629, Optical Techniques in Neurosurgery, Neurophotonics, and Optogenetics, 116292D (5 March 2021); doi: 10.1117/12.2578641



Event: SPIE BiOS, 2021, Online Only

Optoacoustic visualization of GCaMP6f labeled deep brain activity in a murine intracardiac perfusion model

Oleksiy Degtyaruk^{a,b}, Benedict Mc Larney^b, Xosé Luís Deán-Ben^a, Shy Shoham^c, and Daniel Razansky^{a,b*}

^aInstitute for Biomedical Engineering and Institute of Pharmacology and Toxicology, University of Zurich and ETH Zurich, Switzerland

^bInstitute for Biological and Medical Imaging (IBMI), Technical University of Munich and Helmholtz Center Munich, Neuherberg, Germany

^c Tech4Health and Neuroscience Institutes and Department of Ophthalmology, New York University Langone Health, New York, USA *Corresponding author: daniel.razansky@uzh.ch

ABSTRACT

The inability to directly visualize large-scale neural dynamics across the entire mammalian brain in the millisecond temporal resolution regime is among the main limitations of existing neuroimaging methods. Recent advances in optoacoustic imaging systems have led to the establishment of this technology as an alternative method for real-time deep-tissue observations. Particularly, functional optoacoustic neurotomography (FONT) has recently been suggested for three-dimensional imaging of both direct calcium activity and cerebral hemodynamic parameters in rodents. However, the lack of suitable calcium indicators featuring optical absorption peaks within the so-called near-infrared window has hampered the applicability of FONT for imaging neuronal activity deep within the mammalian brain. To surmount this challenge, we developed and validated an intracardially perfused murine brain model labelled with genetically encoded calcium indicator GCaMP6f that closely simulates in vivo conditions. Penetration of light through skull and skin is greatly facilitated after blood is substituted by artificial cerebrospinal fluid (ACSF). The new preparation enabled here the observation of stimulus-evoked calcium dynamics within the mouse brain at penetration depths and spatio-temporal resolution scales not attainable with other neuroimaging techniques.

Keywords: Functional neuroimaging, optoacoustics, calcium dynamics, GCaMP6f, intracardiac perfusion

1. INTRODUCTION

Visualization of neuronal activity across large neuronal populations, including deep and hard-to access areas, with high spatio-temporal resolution is an open quest in neuroscience. To facilitate this, many different imaging approaches to allow non-invasive investigations of neuronal circuits and network functionality have been developed.

Among them, optoacoustic (OA) tomography has shown its capability to image optical absorption deep within highly scattering tissues such as the brain. It provides unique advantages for real-time deep tissue observations at spatio-temporal scales not attainable by other optic imaging modalities, bridging the gab between microscopy and whole brain macroscopy. By relying on ultrasound detection of light-induced signals, it enables non-invasive, highly specific molecular imaging at depths not assessable with conventional optical methods [1,2]. OA brain imaging studies have previously taken advantage of the strong and spectrally distinctive OA contrast provided by oxygenated and deoxygenated hemoglobin to observe oxygenation variations and hemodynamics [3] of stimulus-induced brain function [4,5] or seizure activity deep within the murine brain [6]. Yet relying on hemodynamic observations can only yield indirect representations of neuronal activity. Direct observation of rapid neuronal events in large brain networks is possible through the use of genetically encoded calcium or voltage indicators [7]. In previous studies on zebra fish [8] and mice [9], genetically encoded calcium indicators from the GCaMP-family [10] were shown to be a viable contrast for functional OA neuro-tomography (FONT) capable of capturing fast calcium dynamics. However, due to the peak absorption wavelength of 488 nm used to excite GCaMP, the highly absorbing blood background at this spectral range makes in-vivo imaging beyond superficial cortical areas in mammalian brains difficult. To overcome this limitation, a blood-free excised murine brain model was recently developed [11].

Optical Techniques in Neurosurgery, Neurophotonics, and Optogenetics, edited by V. X. D. Yang, Q. M. Luo, S. K. Mohanty, J. Ding, A. W. Roe, J. M. Kainerstorfer, L. Fu, S. Shoham, Proc. of SPIE Vol. 11629, 116292D · © 2021 SPIE · CCC code: 1605-7422/21/\$21 · doi: 10.1117/12.2578641

Expanding upon this concept, we have developed and validated a GCaMP6f-expressing in situ murine brain model intracardially perfused with artificial cerebrospinal fluid. Capable of imaging calcium dynamics in deep brain regions of the rodent brain with FONT, the model presented here strives to overcame the limitations of low penetrations of light at visible wavelengths by removing the highly absorbing blood background. This preparation is shown to resemble in vivo conditions, demonstrating high viability and functional activity for more than 45 minutes after blood replacement while preserving realistic indicator responses, mimicking in-vivo conditions. Stimulus-induced activity spikes across large parts of the murine brain are detected and validated with EEG and wide-field fluorescence recordings, with large-scale OA recordings performed at penetration depths and spatio-temporal resolution scales not possible with other existing neuroimaging techniques.

2. METHODS

2.1 Perfused mouse model

Six- to twelve-week-old C57BL/6J-Tg(Thyl-GCaMP6f)GP5.5Dkim/J mice (The Jackson Laboratory, United States) were intraperitoneally administered 75U heparin in 100 μ l 0.9 NaCl solution and anaesthetized with a Ketamine (87.5 mg/kg) Xylazine (12.5 mg/kg) mixture. Once the mice reached a stable plane of anesthesia hair-removal cream was used to remove the fur on their head. Animals were placed onto a silicon sheet mounted on a 3D-printed holder at a 4° incline as seen in Figure 1, with the head positioned above an opening covering the FOV of the FONT imaging system. The animal experiments were performed in full compliance with the institutional guidelines of the Helmholtz Center Munich and with approval by the government of Upper Bavaria.

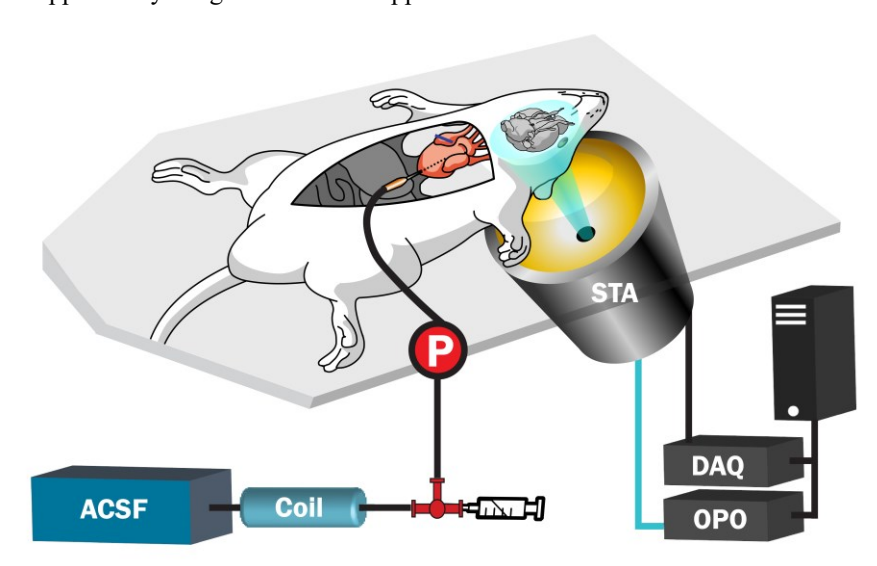


Figure 1. Experimental design for the intracardiac perfused imaging model. ACSF: artificial cerebrospinal fluid; Coil: heating coil; P: pressure transducer; STA: spherical transducer array; OPO: optical parametric oscillator; DAQ: data acquisition unit; PC: personal computer

The mouse head was fixed using a stereotactic mouse head holder (Narishige International Limited, United Kingdom) to avoid motion artifacts. Animals were given a lethal overdose of Ketamine/Xylazine, and following a negative hind paw pinch reflex test their extremities were pinned onto the silicone sheet with 25G needles. Intracardiac perfusion as described in [12] was performed via a perfusion pump (Cole-Parmer, United States) with heated artificial cerebrospinal fluid (ACSF) [13] fumigated with Oxycarbon. ACSF was pumped continuously through a bubble trap connected to a glass heating coil (Radnoti LTD, Ireland) and a physiological pressure transducer (AD Instruments, Australia) connected to a pressure transducer Simulator/Tester (Utah Medical Products, United States). By pumping oxygenated ACSF at 37.5°C (when delivered through the heart with a 25G butterfly needle) at pressures below the physiological limit of 100 mmHg, physiological conditions for the blood-free brain could be established. Oxygenated ACSF was supplied during the entire duration of the experiment to preserve brain functionality and serve as a vehicle for the neuro-stimulating drug Pentylenetetrazol (PTZ) delivery. PTZ (100mg/ml in saline) could be added to the

ACSF flow through a stopcock connected to an Aladdin programmable syringe pump (World Precision instruments, United States), thus inducing fast seizure-like activity in the brain [14].

2.2 EEG data acquisition

A GCaMP6f mouse (n=1) was anaesthetized and given heparin as described above. The scalp was removed and two small openings were made into the skull above both hemispheres 5 mm from each other using a micro drill system (CircuitMedic, United States). The animal was fixed onto the perfusion setup and its head secured in place. EEG-signals were recorded via two custom-made needle electrodes fixed 5 mm apart to a micromanipulator (Narishige International Limited, United Kingdom) and inserted into the drilled holes. Electrodes were connected to a to a DP-311 differential amplifier (Warner Instruments, United States) set to a high pass of 10 Hz, a low pass of 100 Hz and a gain of 100. Amplified signals were digitized via a PowerLab26T data acquisition module (AD Instruments, Australia) and recorded with the Labchart 8 software (AD Instruments, Australia). A grounding electrode connected to the Powerlab DAQ was inserted into the skin around the neck of the mouse, a second one fixed onto the optical table the setup was positioned on. Following 10 min of baseline recording, , a lethal dose of Ketamine/Xylazine-mixture was administered via IP injection and intracardiac perfusion was started as described above. To validate the responsiveness of the brain, 3 ml of PTZ was injected into the perfusion setup over the course of 60 sec. The recorded EEG signals were processed using MatLab (Math Works, United States) by calculating the EEG spectrogram as the short-time Fourier transform with a window of 20 sec, sufficient for detecting higher frequency components in the 10-20 Hz range corresponding to seizure-like activity caused by PTZ.

2.3 Fluorescence data acquisition

Wide-field planar fluorescence recording were performed during perfusion and PTZ stimulations with a Luca R 604 high speed EMCCD camera (Andor Technology, United Kingdom) equipped with a 105 mm Nikon F mount objective (Nikon, Chiyoda, Japan) and a one-inch emission filter with 525 nm center wavelength and 39 nm bandwidth (MF525-39, Thorlabs Inc, United States). GCaMP6f mice (n=2) were anaesthetized, shaved and fixed in place on the silicon layer as described above. The camera was placed below and its position manually adjusted until the head came into focus. The imaged area was illuminated with a single custom-made silica fused-end fiber bundle (CeramOptics GmbH,Germany) positioned below the mouse head and outside of the FOV of the camera. The illumination source was an optical parametric oscillator (OPO)-based laser (EVO I OPO 355nm broadband, Innolas GmbH, Germany) providing short (<10 ns) pulses at 25 Hz with output wavelength set to 488 nm. The acquisition time of the camera was set to 200ms, corresponding to the integration of five laser pulses. The relative fluorescence signal changes (ΔF/F0) were calculated from the recorded images as changes in signal intensity following PTZ injection, corresponding to calcium responses evoked by neural activity. The baseline fluorescence signal level F0 was calculated as the average of frames over 10 seconds preceding the injection.

2.4 Functional optoacoustic neuro-tomography data acquisition

A custom-made matrix transducer array (Imasonic SaS, France) as described here [15] was used to acquire OA data. Detected signals were simultaneously digitized with a custom-made Data Acquisition Unit (Falkenstein Microsysteme, Germany) triggered with the Q-switch output of the tunable OPO laser used for the excitation of OA responses. The STA was placed into the holder at a distance of 0.8 cm from the bottom of the silicon sheet as seen in Figure 1, with the fiber bundle guiding the illumination beam through a central cylindrical aperture. A 3D-printed conical insert with a 2cm diameter top was placed in the space between the silicone sheet and fiber bundle, and 1.5% Agar was poured on top. After the agar hardened, the insert was removed and the opening filled with water to provide acoustic coupling for the optoacoustically-generated ultrasound waves. The fiber bundle delivered light from the output of the OPO laser, which was set to emit alternating pulses of 488 nm / 650 nm light at 25 Hz repetition rate. GCaMP excitation was performed at 488 nm wavelength, while 650 nm served as a control wavelength for which hemoglobin has significantly less optical absorption with GCaMP having no residual absorption. GCaMP6f mice (n=3) were perfused as described above, and OA data was collected through skull and skin during the blood clearing procedure and subsequent PTZ-induced neural activation which commenced after 2 min of perfusion. Volumetric (3D) FONT images were reconstructed from the acquired signals at each wavelength using GPU-based implementation of a backprojection formula [doi:10.1109/TMI.2013.2272079]. The signals were deconvolved with the impulse response of the transducer array elements before reconstruction. In addition, a band-pass filter with cut-off frequencies of 0.1 and 7.5 MHz was applied. Reconstruction of the volumetric image data was performed on a grid of 150x150x100 voxels3 (equivalent to 15x15x10 mm3) to match system's spatial resolution.

3. RESULTS

3.1 Signal changes during intracardiac perfusion

Planar wide-field fluorescence images taken during the blood clearing procedure in a GCaMP6f-labeled mouse are shown in Figure 2A. Vessels can be identified before commencement of the perfusion process, disappearing as blood is removed following 60 sec of perfusion with ACSF. The images appear diffused, affected by the intense scattering of light in the brain and showcasing the limitations of planar fluorescence imaging to surface-weighed 2D visualization. Figure 2B displays normalized fluorescence data time-traces from ROIs in a vessel and an area above the cortex. With the blood background removed, the overall fluorescence signal intensity of the mouse brain increased by 70-130%, however discrimination of signals stemming from different depths was not possible.

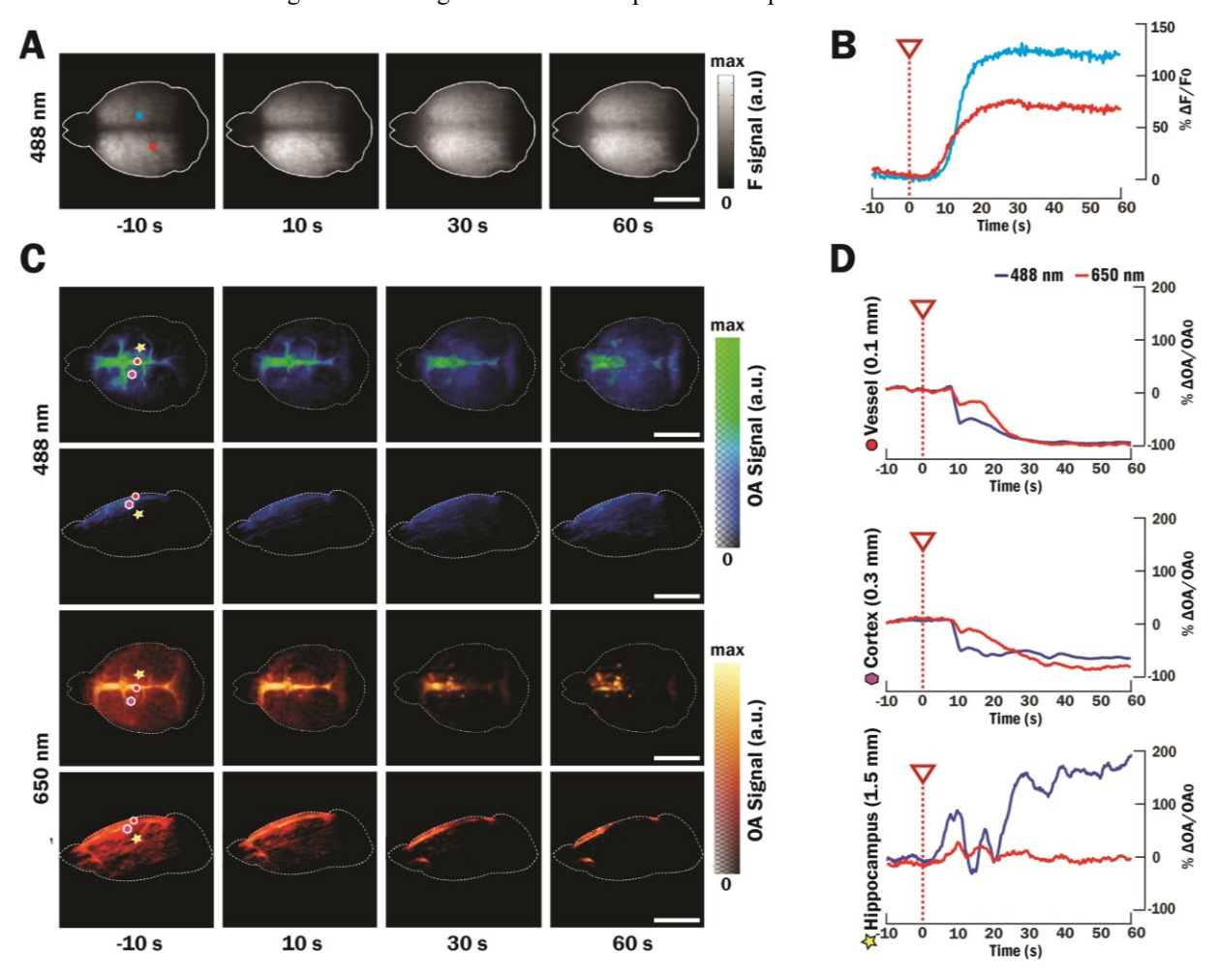


Figure 2. Recorded signal changes during intracardiac perfusion. (A) Planar wide-field fluorescence snapshots during the blood clearing procedure in a GCaMP6f-labeled mouse; Scale bar 5 mm (B) Normalized fluorescence data time-traces from ROIs indicated in panel A. Overall signal intensity increases following blood removal, however planar fluorescence fails to resolve signal changes at different depths. (C) Volumetric FONT images of a GCaMP6f-labeled brain during intracardiac perfusion. As the clearing of blood progresses, signals from vessels shrink while signals from deeper brain areas can be detected with 488 nm excitation. Red dot – Vessel; Purple hexagon – Cortex; Yellow star – Hippocampus.; Scale bar 5 mm (D) Normalized FONT data time-traces recorded during perfusion and averaged over 10 frames are shown from volumes of interest indicated in panel C with the corresponding symbols.

Maximum intensity projections (MIPs) of a GCaMP6f-labeled brain acquired at 488 nm and 650 nm with volumetric FONT during intracardiac perfusion (starting at 0 sec) is shown in Figure 2C along the top and lateral directions. As blood was gradually washed out by ACSF, the background absorption signal declined. This enhanced the effective light penetration and increased the depth at which images could be collected. Before the start of perfusion, signals at the 488 nm wavelength could be extracted at a maximal depth of 1.2-1.5 mm, with the strongest signals stemming from brain vasculature. After clearing the blood for 60 sec, most vessels apart for the rostral confluence of sinuses were blood-free and the maximal depth at which OA signals could be acquired increased to more than 3 mm. Figure 2D shows plots of the relative signals increases as a function of time for selected voxels in the volumetric FONT images marked with corresponding symbols in 2C. In a cortical blood vessel (red circle), the signal was reduced by ~99% at both wavelengths, confirming blood removal. In a cortical area at 0.3 mm depth (purple hexagon) >98% of the 650nm signal disappeared, while only a~50% decrease of the 488 nm signal was observed following perfusion, arguably indicating the presence of GCaMP proteins. In a deeper brain area at 1.5 mm (yellow star), a 200% increase in GCaMP6f-related 488 nm signal was detected after 60 sec of perfusion, indicating an increase in the maximum observable depth thanks to the reduced optical attenuation after clearing.

Unlike the planar fluorescence recordings, FONT was capable of imaging the mouse brain through skin and skull at a high spatial resolution and in 3D, enabling the characterization of signals at different depths. As shown in Figure 3, the background signal was significantly reduced following perfusion with ACSF. More details on the discernible structures in the volumetric FONT images are shown in the transverse and coronal cross-sections along with the corresponding reference images taken from the Allen Mouse Common coordinate Framework [16]. Anatomical structures including both cortical hemispheres and the hippocampus could be distinguished after 60 sec of ACSF perfusion.

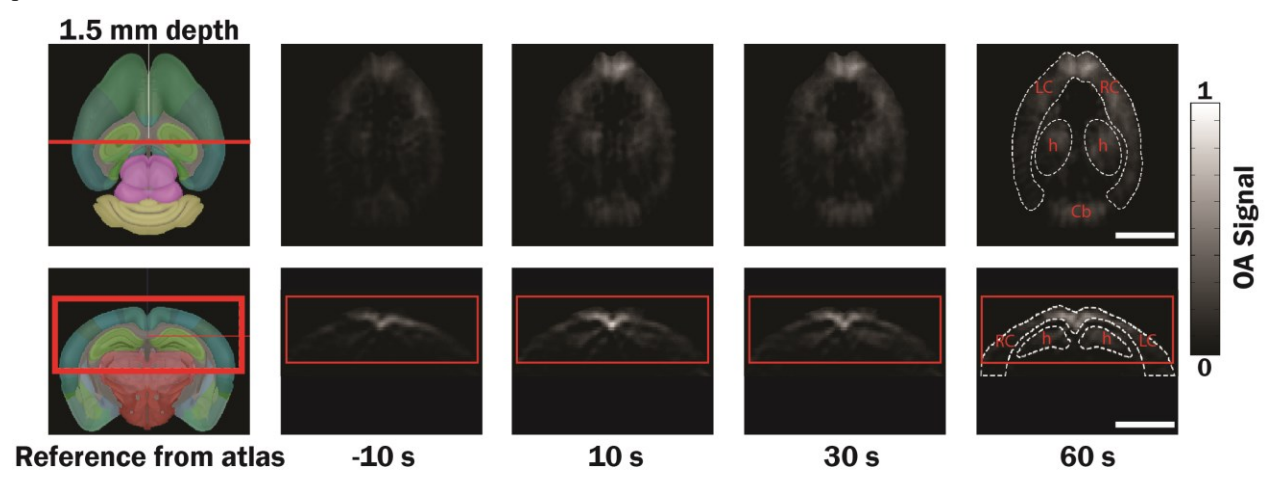


Figure 3. Volumetric FONT recordings from transverse ortho-slices at 1.5 mm depth along with the corresponding coronal slice during intracardiac perfusion. Following 60 sec of blood removal, a median FONT signal increase is observed, making identification of several brain structures possible. L/RC: left/right cortex; h: hippocampus; Cb: Cerebellum. Red lines indicate slice positions for both views; Scale bar 5 mm. Reference images are taken from the Allen Mouse Common coordinate Framework [16]

3.2 Validation of model viability and responsiveness to stimuli

EEG data was acquired in GCaMP6f mice to assess how the perfusion procedure changed neuronal activity profiles and appraise the viability and functionality of the model following blood clearing. Figure 4 displays the power spectra representing the frequency distribution of the brain activity before and after perfusion. Before the perfusion was started signal variations at low frequencies of 3-10 Hz were detected, matching those expected in the *in-vivo* anesthetized brain state. As the perfusion progressed, EEG signal amplitude decreased, forming a new baseline which was recorded for 6 minutes. Injection of PTZ into the perfusion mixture induced neuronal stimulation, represented by an increase in EEG activity. Furthermore, higher frequency signals in the 10-25Hz range corresponding to seizure activity appeared in the frequency distribution. Activity could be detected in the EEG data for up to 45 min after the beginning of perfusion.

Wide-field planar fluorescence recordings in GCaMP6f mice (n=2) were performed to validate neuronal functionality and capability of the model to respond to PTZ stimulation during perfusion. Figure 5A displays a temporal sequence of recorded fluorescence brain activation maps following PTZ injection, resulting in a whole-brain response. Normalized and background-subtracted fluorescence signal traces from areas of interest are seen Figure 5B, indicating PTZ application led to an increase of fluorescence signals of up to 20% over baseline levels. In comparison, no significant changes in fluorescence intensity were detected in control mice (n=3) that received a sham injection with PBS, indicating that signal changes are not due to pressure spikes influencing tissues around brain vessels but due to pharmacological stimulation via PTZ.

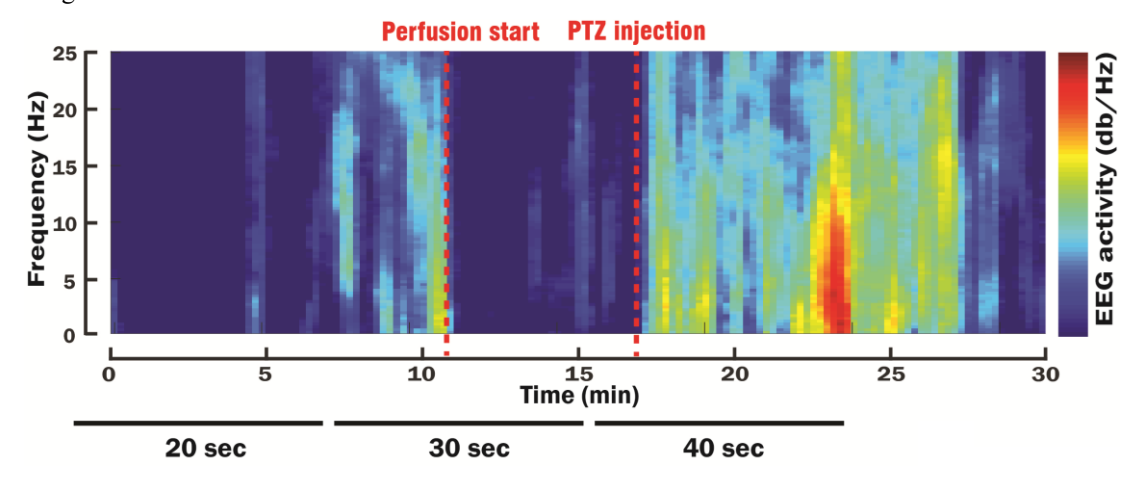


Figure 4. Electroencephalographic (EEG) validation of model viability. The signal power spectra represent the frequency distribution of the brain activity before and after perfusion. Following the addition of Pentylenetetrazol (PTZ) to the perfusion solution, an increase in both signal amplitude and its 10-20 Hz frequency components was detected.

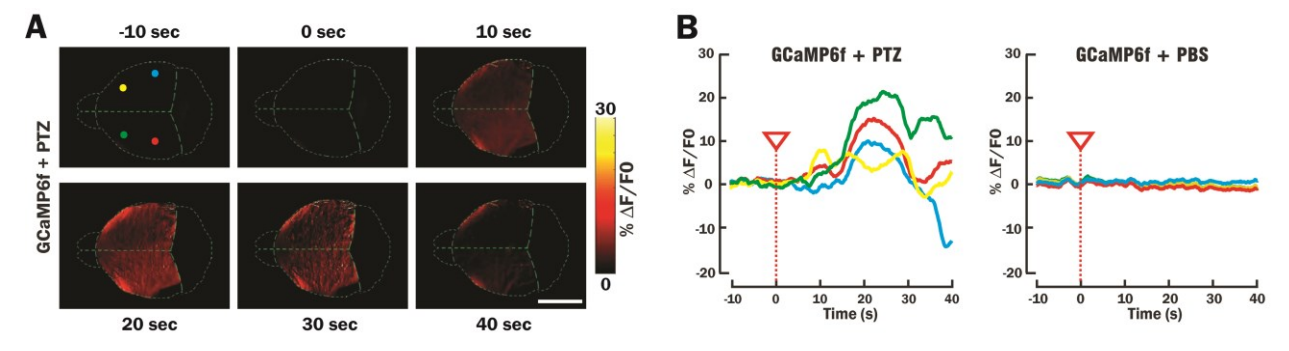


Figure 5. Wide-field planar fluorescence validation of response to Pentylenetetrazol (PTZ) stimulation. (A) Temporal sequence of recorded fluorescence brain activation maps following PTZ injection at 0 seconds; Scale bar 5 mm. (B) Normalized and background-subtracted fluorescence signal traces from areas of interest indicated with colored points in panel A. Signals increased up to 20% over baseline levels in response to PTZ stimulation, while sham injections of PBS induced no changes in fluorescence intensity.

3.3 Observing pharmacologically induced calcium activity with volumetric FONT

Figure 6 presents three-dimensional, observations of calcium changes due to PTZ induced neuronal activation in GCaMP6f-expressing mouse brains with FONT. While multispectral data was acquired, signal increases were only detected in the data acquired at 488 nm. As no significant changes could be observed in the data collected at 650 nm, it is not shown. A detailed visualization of the activated areas is provided in the transverse cross-sections for four different depths displayed in Figure 6A. Following PTZ stimulation, signal changes could be detected up to 3.2 mm depth at 488 nm, allowing data collection from hippocampal areas. At a depth of 4.5 mm, where the mouse line lacks genetically induced GCaMP expression and light at 488 nm might not penetrate, no changes could be observed.

Figure 6B displays single voxel analysis of normalized time traces. In cortical areas at 0.3 mm depth, signal increase of up to 50% at 488 nm compared to baseline levels prior to the start of injection were observed. Analysis of cortex and hippocampal areas at 1.5 mm depth has rendered increases up to 40%. GCaMP6f related signal changes of up to 30% were observed at 3.2 mm depth, more than double what *in-vivo* FONT imaging was capable of in this mouse line.

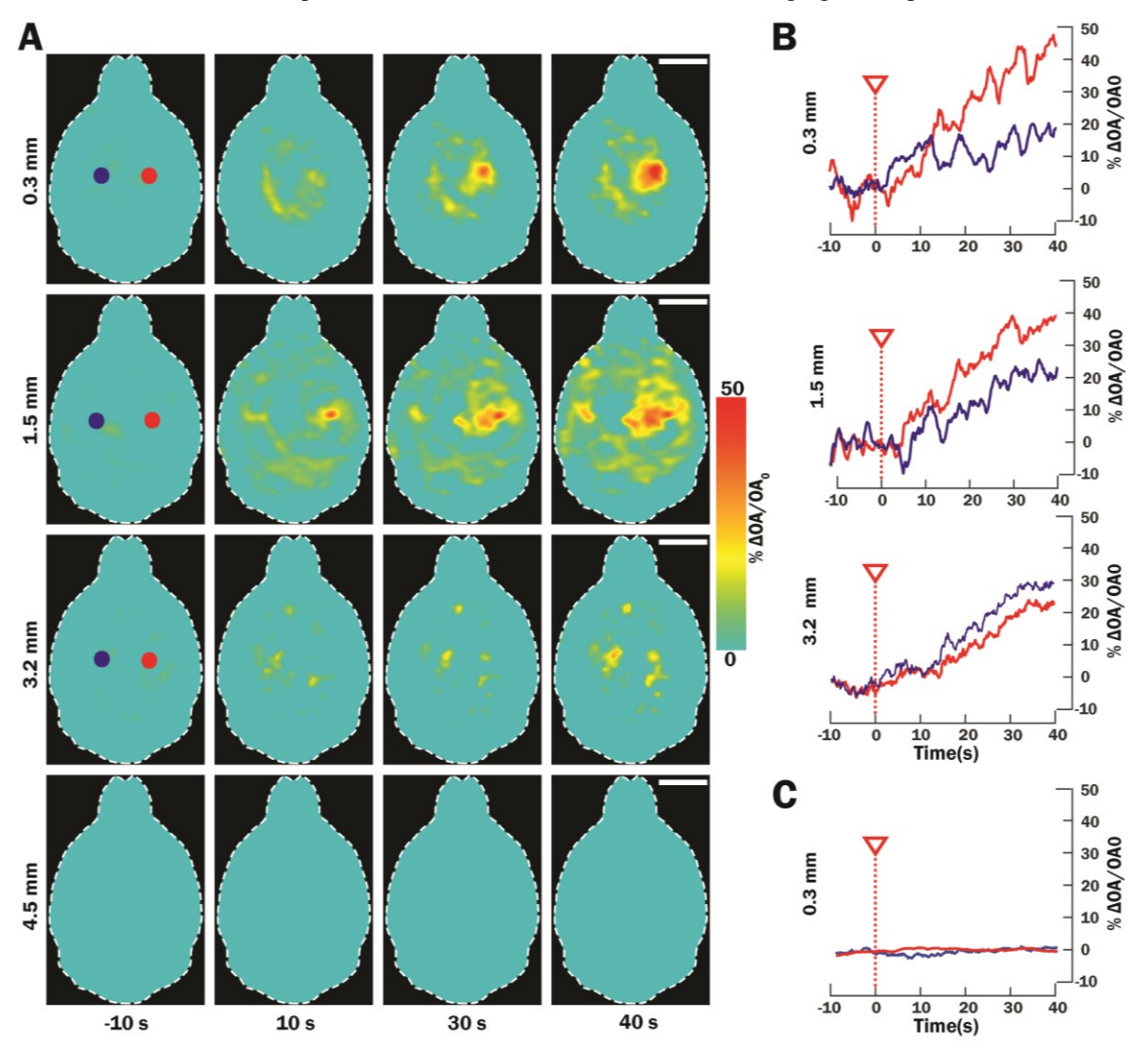


Figure 6. Imaging neuronal activation in a perfused GCaMP6f-expressing mouse at 488 nm with volumetric FONT. (A) Snapshots of relative FONT signal changes over time in four representative slices at different depths induced by PTZ application at 0 seconds; Scale bar 5 mm. Calcium activity signals can be extracted from a depth of up to 3.2 mm in the perfused model, while no signal can be extracted at a depth of 4.5 mm, where no GCaMP6f is expressed. (B) Normalized time-traces of OA signal changes averaged over 10 frames at depths of 0.3 mm, 1.5 mm and 3.2 mm from individual voxels. Corresponding positions are indicated with colored dots in panel A. Red line indicates application of PTZ (C) Normalized time-traces of OA signal changes averaged over 10 frames at depths of 0.3 mm following PBS injection (red line) as a control experiment exhibits no signal changes.

4. CONCLUSION

The presented results demonstrate the possibility and validity of a functional, blood-free *in-situ* mouse brain model for direct tracking of deep calcium dynamics associated with neuronal activity in real time with FONT. By utilizing the cardio-vascular system we were able to remove the highly absorbing blood contrast, enhancing the effective light penetration at 488 nm through skull and skin and increasing the corresponding depth from which GCaMP6f signals could be collected to over 3mm. Brain viability was validated by EEG recordings indicating the presence of neuronal

activity for at least 45 min following the start of perfusion, while stimulus-induced activity spikes across large parts of the murine brain were detected and validated with EEG, wide-field fluorescence and FONT recordings. The whole brain could be efficiently supplied with oxygen and nutrients for more than 45 min following blood clearance, which in combination with physiological pressure and temperature should allow for closer mimicry of *in-vivo* conditions. Since the total duration of the stimulation experiments including the full removal of blood was below 10 min, the data acquired can be attributed to *in-vivo*-like neuronal functionality. Volumetric FONT imaging enabled a clear detection of calcium fluxes as true high-resolution 3D-information not affected by intense light scattering in the brain, while epifluorescence recordings failed to provide high resolution maps of depth-resolved calcium dynamics. The model allows comparisons between *in-vivo* brain data and a blood free *in-situ* preparation, providing a platform to explore the relation between epifluorescence and optoacoustic signals for current and emerging voltage and calcium indicators.

5. ACKNOWLEDGEMENTS

Authors would like to acknowledge their funding sources: European Research Council, grant number ERC-2015-CoG-682379 and the US National Institutes of Health, grants number R21-EY026382 and UF1-NS107680. The authors acknowledge the help of Sven Gottschalk with the design of the study.

REFERENCES

- [1] Prevedel, R., Verhoef, A. J., Pernía-Andrade, A. J., Weisenburger, S., Huang, B. S., Nöbauer, T., Fernández, A., Delcour, J. E., Golshani, P., Baltuska, A. and Vaziri, A., "Fast volumetric calcium imaging across multiple cortical layers using sculpted light," Nature methods 13(12), 1021–1028 (2016).
- [2] Deán-Ben, X. L., Gottschalk, S., Mc Larney, B., Shoham, S. and Razansky, D., "Advanced optoacoustic methods for multiscale imaging of in vivo dynamics," Chemical Society reviews 46(8), 2158–2198 (2017).
- [3] Gottschalk, S., Fehm, T. F., Deán-Ben, X. L. and Razansky, D., "Noninvasive real-time visualization of multiple cerebral hemodynamic parameters in whole mouse brains using five-dimensional optoacoustic tomography," Journal of cerebral blood flow and metabolism: official journal of the International Society of Cerebral Blood Flow and Metabolism 35(4), 531–535 (2015).
- [4] Yao, L., Xi, L. and Jiang, H., "Photoacoustic computed microscopy," Scientific Reports 4, 4960 EP (2014).
- [5] Mc Larney, B., Hutter, M. A., Degtyaruk, O., Deán-Ben, X. L. and Razansky, D., "Monitoring of Stimulus Evoked Murine Somatosensory Cortex Hemodynamic Activity With Volumetric Multi-Spectral Optoacoustic Tomography," Frontiers in neuroscience 14, 536 (2020).
- [6] Gottschalk, S., Fehm, T. F., Deán-Ben, X. L., Tsytsarev, V. and Razansky, D., "Correlation between volumetric oxygenation responses and electrophysiology identifies deep thalamocortical activity during epileptic seizures," Neurophotonics 4(1), 11007 (2017).
- [7] Lin, M. Z. and Schnitzer, M. J., "Genetically encoded indicators of neuronal activity," Nature neuroscience 19(9), 1142–1153 (2016).
- [8] Deán-Ben, X. L., Sela, G., Lauri, A., Kneipp, M., Ntziachristos, V., Westmeyer, G. G., Shoham, S. and Razansky, D., "Functional optoacoustic neuro-tomography for scalable whole-brain monitoring of calcium indicators," Light, science & applications 5(12), e16201 (2016).
- [9] Gottschalk, S., Degtyaruk, O., Mc Larney, B., Rebling, J., Hutter, M. A., Deán-Ben, X. L., Shoham, S. and Razansky, D., "Rapid volumetric optoacoustic imaging of neural dynamics across the mouse brain," Nature Biomedical Engineering 3(5), 392–401 (2019).
- [10] Chen, T.-W., Wardill, T. J., Sun, Y., Pulver, S. R., Renninger, S. L., Baohan, A., Schreiter, E. R., Kerr, R. A., Orger, M. B., Jayaraman, V., Looger, L. L., Svoboda, K. and Kim, D. S., "Ultrasensitive fluorescent proteins for imaging neuronal activity," Nature 499(7458), 295–300 (2013).
- [11] Gottschalk, S., Degtyaruk, O., Mc Larney, B., Rebling, J., Deán-Ben, X. L., Shoham, S. and Razansky, D., "Isolated Murine Brain Model for Large-Scale Optoacoustic Calcium Imaging," Frontiers in neuroscience 13, 290 (2019).

- [12] Gage, G. J., Kipke, D. R. and Shain, W., "Whole animal perfusion fixation for rodents," Journal of visualized experiments: JoVE (65) (2012).
- [13] Bohlen, O. von and Halbach, U., "The isolated mammalian brain: an in vivo preparation suitable for pathway tracing," The European journal of neuroscience 11(3), 1096–1100 (1999).
- [14] Dhir, A., "Pentylenetetrazol (PTZ) kindling model of epilepsy," Current protocols in neuroscience Chapter 9, Unit9.37 (2012).
- [15] Mc Larney, B., Rebling, J., Chen, Z., Deán-Ben, X. L., Gottschalk, S. and Razansky, D., "Uniform light delivery in volumetric optoacoustic tomography," Journal of biophotonics, e201800387 (2019).
- [16] Lein, E. S., Hawrylycz, M. J., Ao, N., Ayres, M., Bensinger, A., Bernard, A., Boe, A. F., Boguski, M. S., Brockway, K. S., Byrnes, E. J., Chen, L., Chen, L., Chen, T.-M., Chi Chin, M., Chong, J., Crook, B. E., Czaplinska, A., Dang, C. N., Datta, S., Dee, N. R., Desaki, A. L., Desta, T., Diep, E., Dolbeare, T. A., Donelan, M. J., Dong, H.-W., Dougherty, J. G., Duncan, B. J., Ebbert, A. J., Eichele, G., Estin, L. K., Faber, C., Facer, B. A., Fields, R., Fischer, S. R., Fliss, T. P., Frensley, C., Gates, S. N., Glattfelder, K. J., Halverson, K. R., Hart, M. R., Hohmann, J. G., Howell, M. P., Jeung, D. P., Johnson, R. A., Karr, P. T., Kawal, R., Kidney, J. M., Knapik, R. H., Kuan, C. L., Lake, J. H., Laramee, A. R., Larsen, K. D., Lau, C., Lemon, T. A., Liang, A. J., Liu, Y., Luong, L. T., Michaels, J., Morgan, J. J., Morgan, R. J., Mortrud, M. T., Mosqueda, N. F., Ng, L. L., Ng, R., Orta, G. J., Overly, C. C., Pak, T. H., Parry, S. E., Pathak, S. D., Pearson, O. C., Puchalski, R. B., Riley, Z. L., Rockett, H. R., Rowland, S. A., Royall, J. J., Ruiz, M. J., Sarno, N. R., Schaffnit, K., Shapovalova, N. V., Sivisay, T., Slaughterbeck, C. R., Smith, S. C., Smith, K. A., Smith, B. I., Sodt, A. J., Stewart, N. N., Stumpf, K.-R., Sunkin, S. M., Sutram, M., Tam, A., Teemer, C. D., Thaller, C., Thompson, C. L., Varnam, L. R., Visel, A., Whitlock, R. M., Wohnoutka, P. E., Wolkey, C. K., Wong, V. Y., Wood, M., Yaylaoglu, M. B., Young, R. C., Youngstrom, B. L., Feng Yuan, X., Zhang, B., Zwingman, T. A. and Jones, A. R., "Genome-wide atlas of gene expression in the adult mouse brain," Nature 445, 168 EP - (2006).